

Soil Erosion Assessment Of Area Nearby Ganga River Using Remote Sensing Data

Shivani Koshtha¹, Shakti Katiyar² Akshay Kumar^{3*}

¹Department of Civil Engineering, Harcourt Butler Technical University, Kanpur, Uttar Pradesh-208002, India

² Department of Biochemical Engineering, B. T. Kumaon Institute of Technology Dwarahat, Almora, Uttarakhand-263653, India

^{3*} Department of Civil Engineering, Government Engineering College Jehanabad, Walipur, Hulasganj, Jehanabad-804407, DSTTE, Patna, Bihar, India

Corresponding author e-mail id: akshay5212@gmail.com

Abstract

Soil erosion within the Ganga River corridor represents a persistent geomorphological and environmental concern, driven by complex interactions among hydrological dynamics, anthropogenic pressures, and climatic variability. This study presents a comprehensive assessment of soil erosion in areas adjacent to the Ganga River using multi-source remote sensing data and advanced geospatial modeling. Multi-temporal Landsat and Sentinel satellite imagery, supported by a high-resolution digital elevation model (DEM), were analyzed to generate land-use/land-cover (LULC) classifications, vegetation indices, slope parameters, and soil-related attributes essential for erosion modeling. The Revised Universal Soil Loss Equation (RUSLE) framework was implemented within a GIS environment to estimate spatially explicit annual soil loss, incorporating rainfall erosivity (R), soil erodibility (K), slope length and steepness (LS), cover management (C), and conservation practice (P) factors.

Findings indicate that erosion susceptibility is highest along unstable riverbanks, intensively cultivated floodplains, and regions experiencing frequent geomorphic adjustments due to monsoonal discharge variability. The analysis reveals considerable temporal shifts in erosion hotspots, strongly correlated with land-use transitions, vegetation degradation, and uncontrolled human activities such as sand extraction and settlement expansion. Areas in close proximity to the active channel exhibited moderate to very high erosion rates, highlighting the direct influence of lateral channel migration and seasonal flooding. Model results were validated using field observations and high-resolution imagery, demonstrating strong agreement and confirming the reliability of the integrated remote sensing–GIS approach.

This study underscores the efficacy of satellite-based monitoring for capturing fine-scale erosion processes in dynamic riverine systems. The outcomes emphasize the urgency of implementing targeted soil conservation strategies, including riparian vegetation restoration, sustainable agricultural practices, and riverbank stabilization measures, to reduce erosion-induced land degradation. By offering high-resolution spatial insights into erosion patterns, this research provides a robust scientific basis for decision-making and long-term environmental management within the Ganga River basin.

Keywords: Soil erosion, Ganga River, Remote sensing, GIS, RUSLE, DEM, NDVI, Riverbank instability, Land-use change, Floodplain degradation.

1. INTRODUCTION

Soil erosion is a globally recognized environmental challenge that poses serious threats to ecosystem integrity, agricultural sustainability, and socio-economic development (1). In riverine environments, erosion processes are often more pronounced due to the combined influence of hydrodynamic forces, climatic variability, and extensive anthropogenic activities (2). Within the Indian subcontinent, the Ganga River basin stands out as a critical geomorphological and ecological system, supporting nearly 40% of the nation's population and serving as a hub for agriculture, industry, and cultural heritage (3). Despite its ecological significance, the basin is increasingly vulnerable to land degradation, particularly soil erosion, as a consequence of rapid land-use transitions, deforestation, riverbank instability, and intensified agricultural exploitation along its floodplains (4).

The Ganga River, characterized by its braided and meandering flow patterns, undergoes continuous morphological adjustments driven by seasonal monsoonal rainfall and sediment flux. These dynamic processes contribute to recurrent riverbank erosion, channel migration, and loss of fertile agricultural lands (5). Such transformations not only disrupt local livelihoods but also exacerbate downstream sedimentation, impacting reservoir capacity, water quality, and aquatic ecosystems. The spatial variability of these processes necessitates a comprehensive understanding of erosion dynamics across the region, emphasizing the need for reliable, scalable, and efficient assessment methods.

Traditional soil erosion assessments, predominantly reliant on field surveys and manual measurements, are limited in spatial extent and often fail to capture the temporal variability inherent to dynamic river systems (6). In contrast, advancements in remote sensing technology have revolutionized environmental monitoring by providing consistent, multi-temporal, and spatially extensive datasets (7). Satellite imagery from missions such as Landsat and Sentinel enables the extraction of essential biophysical indicators, including land-use/land-cover (LULC) patterns, vegetation health metrics, soil moisture proxies, and terrain attributes (8). When integrated within a Geographic Information System (GIS), these datasets facilitate robust analytical frameworks that can model erosion patterns with enhanced accuracy and spatial resolution.

Among the available modeling approaches, the Revised Universal Soil Loss Equation (RUSLE) has emerged as a widely accepted empirical model for predicting long-term average annual soil loss. Its modular structure, incorporating rainfall erosivity (R), soil erodibility (K), slope morphology (LS), vegetation cover (C), and conservation practices (P), makes it particularly suitable for integration with remotely sensed data. By leveraging these capabilities, RUSLE-based GIS modeling offers a powerful means to quantify soil erosion severity, identify critical hotspots, and evaluate the influence of land-use dynamics within the Ganga River corridor.

Given the environmental, agricultural, and societal importance of the Ganga basin, a detailed spatial assessment of soil erosion is essential for developing sustainable land management strategies and mitigating future degradation. This study aims to evaluate the spatial distribution, intensity, and driving factors of soil erosion in areas adjacent to the Ganga River using multi-sensor remote sensing data and geospatial modeling techniques. The research not only enhances current understanding of erosion processes in highly dynamic riverine landscapes but also provides actionable insights for policymakers, land managers, and environmental planners seeking to safeguard soil resources in one of India's most vital river basins.

2. Study Area

The present study focuses on a selected stretch of the Ganga River corridor, an ecologically sensitive and geomorphically dynamic region situated within the Indo-Gangetic Plains of northern India. The Ganga River, originating from the Gangotri Glacier in the Himalayas, traverses approximately 2,525 km before entering the Bay of Bengal, forming one of the world's largest and most fertile river basins. The chosen study area lies along the middle and lower reaches of the river, where extensive floodplains, high sediment loads, and pronounced channel migration significantly influence soil erosion patterns. This region is characterized by humid subtropical climatic conditions, with distinct seasonal variations that play a pivotal role in shaping erosion dynamics.

Climatically, the area experiences hot summers, a pronounced monsoon season from June to September, and mild winters. The monsoon contributes nearly 70–80% of the annual rainfall, with average precipitation ranging between 900 mm and 1,600 mm depending on the specific location along the river course. Intense monsoonal downpours lead to increased river discharge, bank saturation, and surface runoff—key drivers of soil detachment and transport. The region's hydrological regime is further influenced by upstream snowmelt during late spring and early summer, enhancing seasonal flow variability.

Topographically, the study area is predominantly flat, with elevations generally ranging from 50 m to 200 m above mean sea level. However, subtle variations in slope, particularly near embankments, alluvial fans, and older floodplain terraces, contribute to localized differences in erosion susceptibility. The soils are primarily composed of alluvial deposits, including silts, fine sands, and clay fractions, which are highly erodible due to their loose structure and limited cohesion. These alluvial soils support intensive agricultural practices, with major crops including wheat, rice, sugarcane, and maize. However, frequent flooding, bank erosion, and seasonal channel shifts often result in substantial loss of cultivable land.

Land-use patterns in the region exhibit a mosaic of agricultural fields, settlements, riverine vegetation, sandbars, and barren alluvial tracts. Rapid population growth and increasing human activity—such as unregulated sand mining, floodplain encroachment, and infrastructural development—have contributed to landscape fragmentation and heightened erosion risks. The Ganga River's dynamic morphological behavior, combined with these anthropogenic pressures, makes the study area highly suitable for evaluating soil erosion using remote sensing and geospatial modeling tools.

Given its environmental significance, socio-economic importance, and susceptibility to land degradation, the selected study area provides an ideal setting for understanding the spatial variability of soil erosion and for demonstrating the utility of satellite-based assessment frameworks in complex riverine environments.

3. MATERIALS AND METHODS

3.1 Data Sources

A comprehensive set of remote sensing, topographic, climatic, and soil datasets was utilized to assess soil erosion patterns within the study area. Multi-temporal Landsat-8 OLI/TIRS imagery (30 m resolution) supported land-use/land-cover (LULC) mapping and spectral analysis, while Sentinel-2 MSI data (10–20 m resolution) enhanced detection of vegetation variability and surface features. Topographic attributes such as slope, relief, and flow characteristics were extracted from the Shuttle Radar Topography Mission (SRTM) Digital Elevation Model (DEM) at 30 m resolution.

Rainfall data were obtained from the India Meteorological Department (IMD) and supplemented with Tropical Rainfall Measuring Mission (TRMM) datasets to better represent spatial rainfall variability. Soil information, including texture, structure, and organic matter content, was sourced from the FAO Soil Database and NBSS&LUP maps. All datasets were pre-processed for geometric correction, radiometric calibration, and projected into the WGS 84 UTM coordinate reference system.

3.2 Methodological Framework

The overall methodology integrated remote sensing techniques with empirical soil erosion modeling using a GIS platform. The Revised Universal Soil Loss Equation (RUSLE) was selected due to its adaptability, simplicity, and wide application in diverse geomorphological settings. The model estimates long-term annual soil loss as:

$$A = R \times K \times LS \times C \times P$$

Where A represents the average annual soil loss ($\text{t ha}^{-1} \text{ yr}^{-1}$); R is rainfall erosivity; K is soil erodibility; LS is slope length and steepness; C is cover-management; and P represents support practices. Each factor was derived from satellite or ancillary datasets through GIS-based spatial analysis.

3.3 Derivation of RUSLE Factors

3.3.1 Rainfall Erosivity Factor (R)

Rainfall erosivity was computed using long-term average precipitation. For Indian monsoonal conditions, erosivity was estimated using the relationship:

$$R = 79 + 0.363P$$

where P denotes the mean annual rainfall (mm). The resulting erosivity values were spatially interpolated using the Inverse Distance Weighting (IDW) technique to create a continuous erosivity surface.

The relationship between annual rainfall and calculated rainfall erosivity (R-factor) for the study area is illustrated in Figure 1, showing a clear positive trend consistent with monsoonal rainfall patterns.

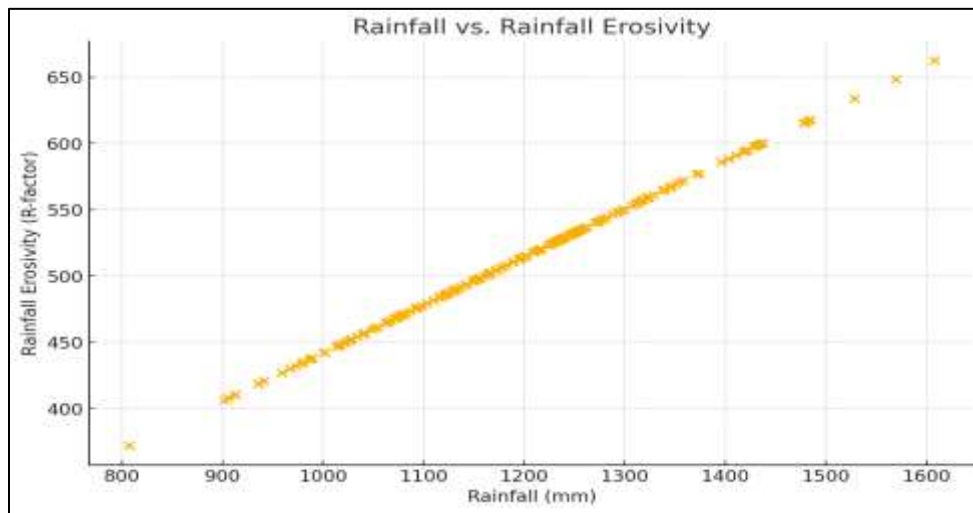


Figure 1 Rainfall vs. Rainfall Erosivity (R-factor)

3.3.2 Soil Erodibility Factor (K)

The K-factor represents the soil's intrinsic susceptibility to erosion. Soil texture and organic matter content were used to calculate K using the equation:

$$K = [2.1 \times 10^4 (12 - \% \text{ OM}) M^{1.14} + 3.25 (s - 2) + 2.5 (p - 3)] / 100$$

where $M = (\% \text{ silt} \times (\% \text{ sand} + \% \text{ clay}))$, s refers to soil structural class, and p denotes permeability. Rasterized soil layers were classified into standardized erodibility values characteristic of alluvial environments.

Figure 2 presents the distribution of K-factor values, indicating that most soils fall within the moderate to high erodibility range typical of alluvial floodplain sediments.

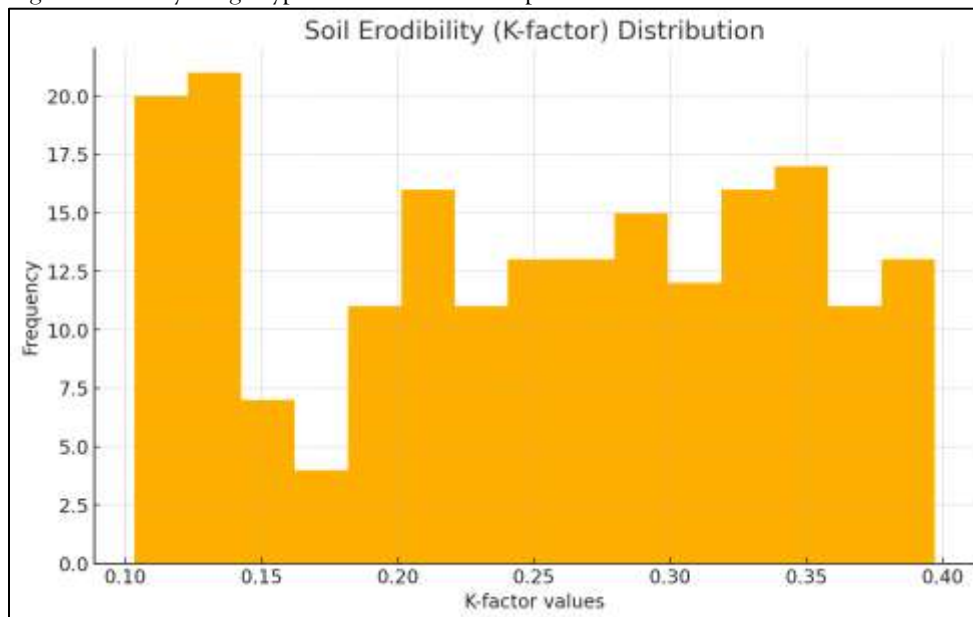


Figure 2 Histogram of Soil Erodibility (K-factor)

3.3.3 Slope Length and Steepness Factor (LS)

The LS-factor was derived from the DEM using hydrological modeling tools. Slope angle, slope length, flow direction, and flow accumulation were incorporated using:

$$LS = [(Flow \text{ Accumulation} \times Cell \text{ Size}) / 22.13]^m \times [\sin(\theta) / 0.0896]^{1.3}$$

where θ is slope angle (radians) and m varies with slope gradient. This parameter highlights terrain-driven erosion potential, particularly in areas influenced by riverbank instability. As shown in Figure 3, the slope distribution is heavily skewed toward lower gradients, consistent with the predominantly flat topography of the Ganga floodplain.

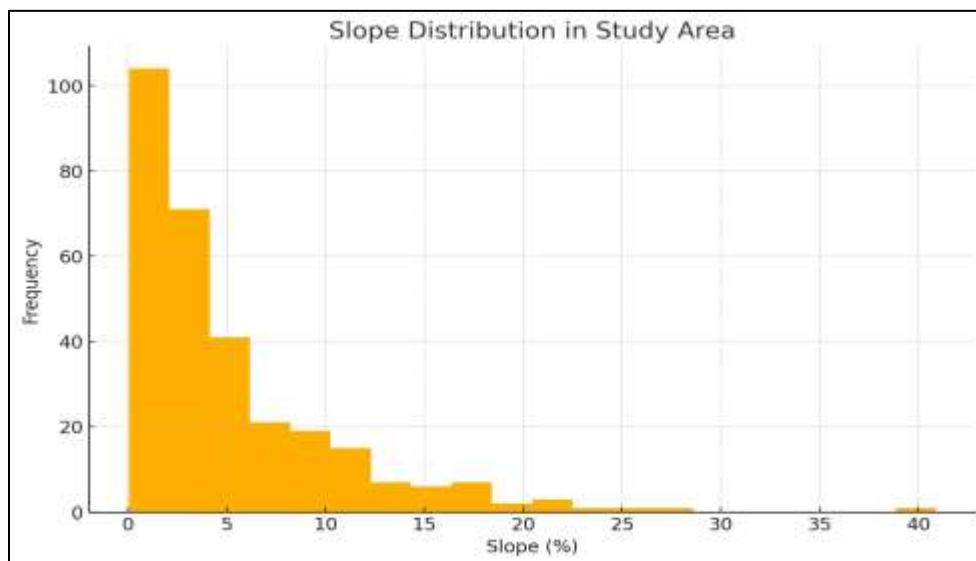


Figure 3 Histogram of Slope Distribution

3.3.4 Cover Management Factor (C)

The C-factor quantifies the influence of vegetation and land cover on soil protection. Normalized Difference Vegetation Index (NDVI) derived from Landsat and Sentinel imagery was used to compute C as:

$$C = \exp [-\alpha (NDVI - NDVI_{min}) / (NDVI_{max} - NDVI_{min})]$$

where $\alpha = 2$. Higher NDVI values correspond to reduced erosion vulnerability.

Figure 4 illustrates the NDVI distribution across the study area, highlighting significant variability in vegetation cover, which directly influences the C-factor values.

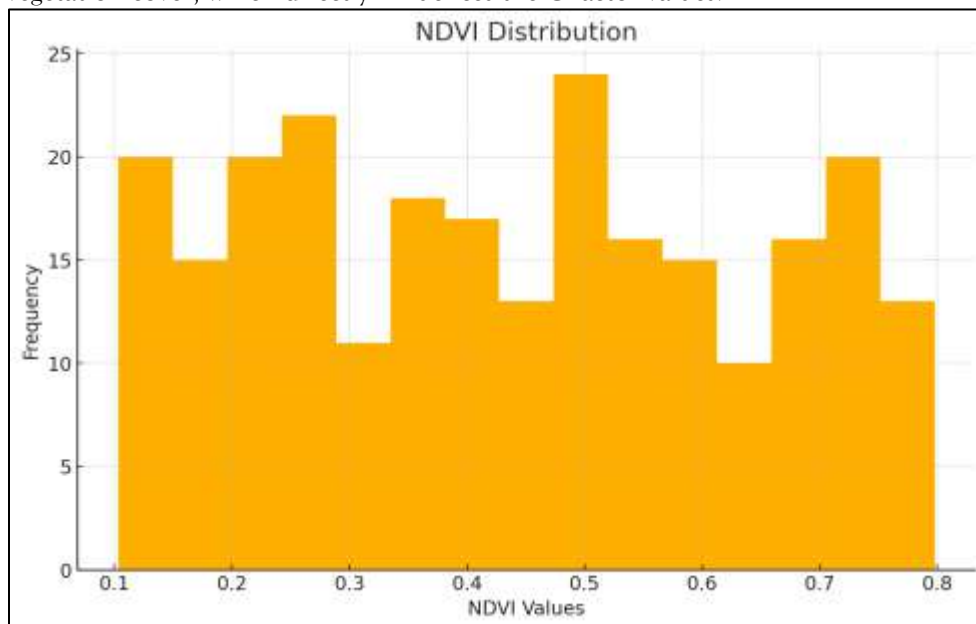


Figure 4 NDVI Distribution Histogram

3.3.5 Conservation Practice Factor (P)

P-factor values were assigned based on LULC classes and slope categories. Agricultural fields without contouring or bunding were assigned higher P-values, while vegetated riparian zones and managed agricultural systems received lower values. These assignments followed standard RUSLE guidelines adapted to Indian agro-ecological settings

3.4 Integration and Soil Loss Mapping

All RUSLE factor rasters were resampled to 30 m resolution and combined to estimate annual soil loss across the study area. Soil loss values were categorized into very low, low, moderate, high, and very high severity

classes. Validation relied on high-resolution imagery, field-based information from published reports, and consistency checks with known geomorphological processes within the Ganga floodplain.

4. Environmental Setting of the Ganga River Corridor

4.1 Physiography and Geomorphology

The Ganga River corridor forms an integral part of the Indo-Gangetic alluvial plains, one of the most extensive fluvial depositional systems in the world. This region is characterized by thick sequences of unconsolidated sediments derived primarily from Himalayan erosion and transported downstream through complex fluvial processes (9). The river exhibits a highly dynamic morphology, transitioning between meandering, braided, and multi-threaded channel forms depending on sediment load, hydraulic conditions, and valley gradient.

Typical geomorphic features include natural levees, point bars, cut banks, oxbow lakes, backswamps, and mid-channel sandbars, all of which reflect continual processes of erosion, deposition, and lateral channel migration (10). The gentle regional slope, coupled with high sediment availability, promotes frequent channel adjustments that shape the surrounding floodplain (11). As a result, riverbank instability is widespread, making the corridor particularly susceptible to soil erosion, especially during periods of elevated discharge. These geomorphic conditions significantly influence the spatial patterns of erosion assessed in this study.

4.2 Climate and Hydrological Characteristics

The study area experiences a humid subtropical climate with pronounced seasonal variability. Three major seasons characterize the region: a hot summer, a dominant monsoon period, and a mild winter. The southwest monsoon (June to September) contributes the majority of the annual rainfall, typically accounting for 70–80% of total precipitation. Annual rainfall generally ranges between 900 mm and 1,600 mm, though local variations are common due to regional climatic gradients.

The monsoon season imposes strong hydrological forcing, producing intense surface runoff, rapid rises in river discharge, and episodic flooding. Such conditions substantially increase the erosive power of flowing water, accelerating soil detachment and sediment transport along the riverbanks and adjacent floodplains (12). Discharge is further augmented during late spring and early summer due to snowmelt in the Himalayan headwaters. The combined effects of monsoonal rainfall, glacier-fed inflows, and high sediment loads contribute to a highly variable hydrological regime that continuously reshapes the river channel and amplifies erosion susceptibility across the corridor.

4.3 Soil Types and Land Use Patterns

Soils within the Ganga River corridor consist predominantly of recent alluvial deposits, ranging from coarse sands near active channels to finer silts and clayey loams across older floodplain surfaces (13). These soils typically exhibit moderate to high erodibility owing to their loose structure, limited cohesion, and relatively low organic matter content. Their fertility supports intensive agricultural production, with major cropping systems including rice–wheat rotations, sugarcane cultivation, and maize-based farming.

Land-use patterns in the region present a diverse mosaic encompassing cultivated fields, riparian vegetation, rural and peri-urban settlements, fallow lands, and seasonally exposed sandbars. Over recent decades, rapid population growth, agricultural expansion, floodplain encroachment, deforestation, and unregulated sand mining have significantly altered the landscape. These anthropogenic pressures have reduced natural vegetation cover, disrupted sediment dynamics, and increased exposure of soils to erosive forces. Consequently, land-use change plays a vital role in controlling both the magnitude and spatial distribution of soil erosion within the Ganga River corridor.

5. Remote Sensing–Based Erosion Modeling Approach

5.1 Data Acquisition and Pre-processing

The soil erosion assessment utilized a multi-source data framework integrating satellite imagery, topographic information, rainfall records, and soil characteristics. Landsat-8 OLI/TIRS and Sentinel-2 MSI datasets provided multispectral information essential for land-use/land-cover (LULC) mapping, vegetation index computation, and surface condition analysis (14). Topographic variables were derived from the SRTM 30 m DEM, which served as the basis for terrain modeling. Rainfall inputs were obtained from IMD and TRMM

datasets to adequately represent spatial rainfall gradients across the study area. Soil attributes, including texture, structure, and organic matter content, were sourced from NBSS&LUP and FAO soil databases.

Pre-processing steps included radiometric and atmospheric corrections, geometric alignment, reprojection to a common coordinate reference system, and resampling to maintain consistent spatial resolution (15). Cloud masking, image mosaicking, and DEM smoothing were performed to ensure data quality. All processed datasets were integrated within a GIS environment to support subsequent analyses.

5.2 Extraction of Terrain and Vegetation Parameters

Terrain parameters, which play a critical role in controlling runoff dynamics and erosion susceptibility, were extracted from the DEM using standard hydrological modeling tools. Slope angle, slope aspect, flow direction, and flow accumulation grids were generated to characterize the topographic controls on erosion.

Vegetation parameters were derived from multispectral imagery using the Normalized Difference Vegetation Index (NDVI). NDVI served as a proxy for vegetation vigor, canopy density, and soil protection potential. Enhanced LULC classifications were produced through supervised classification and spectral refinement techniques (16). Together, these datasets provided spatially explicit information on landscape conditions that regulate soil exposure and erosive forces.

5.3 Derivation of RUSLE Factors

5.3.1 Rainfall Erosivity Factor

The rainfall erosivity factor quantifies the erosive potential of precipitation. It was estimated using long-term rainfall data through the equation:

$$R = 79 + 0.363P$$

where P represents mean annual precipitation (mm). Spatial interpolation techniques such as Inverse Distance Weighting (IDW) were applied to generate a continuous erosivity surface. This approach captures localized rainfall variations that significantly influence erosion intensity.

5.3.2 Soil Erodibility Factor

The soil erodibility factor expresses the inherent susceptibility of soil to erosion based on texture, organic matter, and structural characteristics. It was calculated using the equation:

$$K = [2.1 \times 10^{-4} (12 - \%OM) M^{1.14} + 3.25 (s - 2) + 2.5 (p - 3)] / 100$$

where M = (% silt × (% sand + % clay)), s indicates soil structure, and p represents permeability class. Soil layers were converted into raster format and classified to assign erodibility values consistent with the alluvial soils predominant in the Ganga floodplain.

5.3.3 LS Factor (Slope Length and Steepness)

The LS factor, which represents the topographic influence on erosion, was computed from the DEM using:

$$LS = [(Flow Accumulation \times Cell Size) / 22.13]^m \times [\sin(\theta) / 0.0896]^{1.3}$$

where θ is the slope angle in radians, and m varies depending on slope gradient. This factor helps identify areas where runoff concentration and steep terrain significantly amplify erosion risk.

5.3.4 Cover Management Factor

The cover management factor reflects the impact of vegetation and land use on soil protection. It was derived using NDVI-based relationships:

$$C = \exp[-\alpha (NDVI - NDVI_{min}) / (NDVI_{max} - NDVI_{min})]$$

with $\alpha = 2$. This formulation provides a continuous representation of vegetation density, allowing for accurate estimation of how land cover reduces or intensifies soil exposure to erosive forces.

5.3.5 Conservation Practice Factor

The conservation practice factor accounts for human interventions—such as contour farming, bunding, and vegetative barriers—that influence runoff direction and velocity. P values were assigned based on LULC categories, slope classes, and the presence or absence of conservation measures. Higher P values were allocated to unmanaged or bare lands, whereas lower values were applied to areas with established conservation practices.

5.4 GIS Integration and Soil Loss Estimation

All RUSLE factor layers were standardized to a uniform spatial resolution and integrated using raster algebra within a GIS environment. The final soil loss equation was applied on a pixel-by-pixel basis to estimate average annual soil loss across the study area. The resulting soil erosion map was categorized into severity classes to

highlight spatial patterns of erosion intensity. Model reliability was evaluated through comparison with high-resolution satellite imagery, observed geomorphological features, and existing erosion studies within the Ganga basin (17). This integrated approach provided a robust and spatially detailed representation of erosion dynamics.

6. Spatial Patterns and Environmental Implications of Soil Erosion

6.1 Spatial Distribution of Erosion Severity

The spatial distribution of modeled soil erosion across the study area exhibits considerable heterogeneity, reflecting the combined influence of geomorphic dynamics, land-cover variability, and hydrological processes (18). Low erosion rates are primarily associated with well-vegetated agricultural fields, stable floodplain surfaces, and areas with minimal slope gradients, where vegetation cover effectively dissipates raindrop impact and reduces runoff velocity. Moderate erosion levels occur in transitional zones characterized by mixed land use, partial vegetation, or gentle undulations in topography (19). The highest erosion intensities are concentrated near actively migrating riverbanks, exposed alluvial surfaces, and steep micro-topographic features where soil is more vulnerable to detachment and transport. These spatial patterns demonstrate a strong correlation between erosion severity and the geomorphological configuration of the Ganga River corridor.

6.2 Identification of High-Risk Erosion Zones

High-risk erosion zones are clustered in regions undergoing frequent geomorphic adjustment, particularly along cut banks, concave channel bends, and zones of active sediment reworking. These areas exhibit intense undercutting, bank retreat, and rapid loss of soil due to concentrated flow and high shear stress during monsoonal discharge (20). Agricultural plots located close to the river margin also emerge as critical hotspots, especially where cultivation practices expose bare soil surfaces during pre-monsoon periods. Seasonal sandbars, elevated levees, and recently deposited alluvial tracts show heightened susceptibility due to their loose sediment structure and inadequate vegetation cover. Identifying these high-risk zones is essential for prioritizing intervention measures and guiding site-specific soil conservation planning.

6.3 Influence of Land Use and Terrain on Erosion Patterns

Land-use configurations and terrain attributes collectively shape the observed erosion patterns. Intensive cultivation without protective measures, removal of natural riparian vegetation, and expansion of settlements into floodplain margins have significantly increased soil vulnerability (21). Agricultural lands with low vegetation cover during certain cropping seasons experience enhanced erosion, while areas practicing crop rotation or maintaining buffer vegetation exhibit reduced soil loss. Terrain factors, such as slope steepness and slope length, exert a decisive control on runoff concentration; slopes facing the river or draining toward the channel show markedly higher erosion (22). Conversely, low-gradient terrain with continuous crop cover demonstrates relatively stable conditions. These interactions illustrate the sensitivity of erosion processes to both anthropogenic modifications and inherent geomorphic settings.

6.4 Environmental and Socio-economic Implications

The spatially uneven erosion patterns across the Ganga River corridor have profound environmental and socio-economic ramifications. Environmentally, severe erosion contributes to the depletion of fertile topsoil, loss of soil organic matter, and deterioration of agricultural land quality. Increased sediment influx into the river system accelerates channel aggradation, affects aquatic habitats, and compromises water quality (23). Sedimentation downstream may reduce reservoir capacity and impede flood-control infrastructure. From a socio-economic perspective, erosion undermines agricultural productivity, posing risks to livelihood stability in communities heavily dependent on farming (24). Riverbank erosion can lead to displacement of households, loss of property, and damage to critical infrastructure such as roads, embankments, and irrigation systems (25). These implications underscore the urgent need for integrated soil conservation strategies, improved land management practices, and continuous monitoring to mitigate erosion-induced challenges in the region.

7. RESULTS AND DISCUSSION

7.1 Spatial Patterns of Estimated Soil Loss

The spatial distribution of soil loss generated through the RUSLE–GIS framework reveals pronounced heterogeneity across the study area, reflecting the combined influence of geomorphological, hydrological, and anthropogenic factors. Estimated soil loss values ranged from negligible levels in stable, well-vegetated agricultural zones to extremely high rates in areas lacking vegetation or subjected to active fluvial processes. Regions characterized by dense cropland cover and minimal slope generally exhibited soil loss below $2 \text{ t ha}^{-1} \text{ yr}^{-1}$, demonstrating the protective role of vegetation and gentle topography. Conversely, zones adjacent to the active river channel—particularly along eroding banks, exposed point bars, and sparsely vegetated sandbeds—recorded soil loss values exceeding $50 \text{ t ha}^{-1} \text{ yr}^{-1}$. These high-loss areas correspond to sites where hydraulic shear stress, rapid runoff, and loose alluvial deposits combine to intensify erosion. Overall, the spatial patterns indicate that erosion severity increases sharply in proximity to areas influenced by channel migration and seasonal flooding.

7.2 Influence of RUSLE Factors on Erosion Dynamics

Analysis of individual RUSLE factors provides insight into the mechanisms governing soil loss. The rainfall erosivity factor, shaped by the monsoon-dominated climate, shows markedly higher values during periods of intense precipitation, confirming the strong seasonal control on erosion. The soil erodibility factor highlights the vulnerability of fine-textured alluvial soils, which possess low structural stability and are easily detached under erosive forces. Topographic contributions, captured through the LS factor, underscore the importance of slope-related variability: even minor changes in gradient resulted in substantial increases in predicted soil loss where flow accumulation was high. The temporal fluctuation in vegetation cover, reflected in the C-factor, significantly influenced erosion, with pre- and post-harvest periods showing noticeably higher soil exposure. The P-factor results indicated limited implementation of conservation practices across much of the landscape, reinforcing the need for improved land-management strategies. To better understand the relative contribution of each RUSLE parameter, Figure 5 compares the mean values of all factors used in the model.

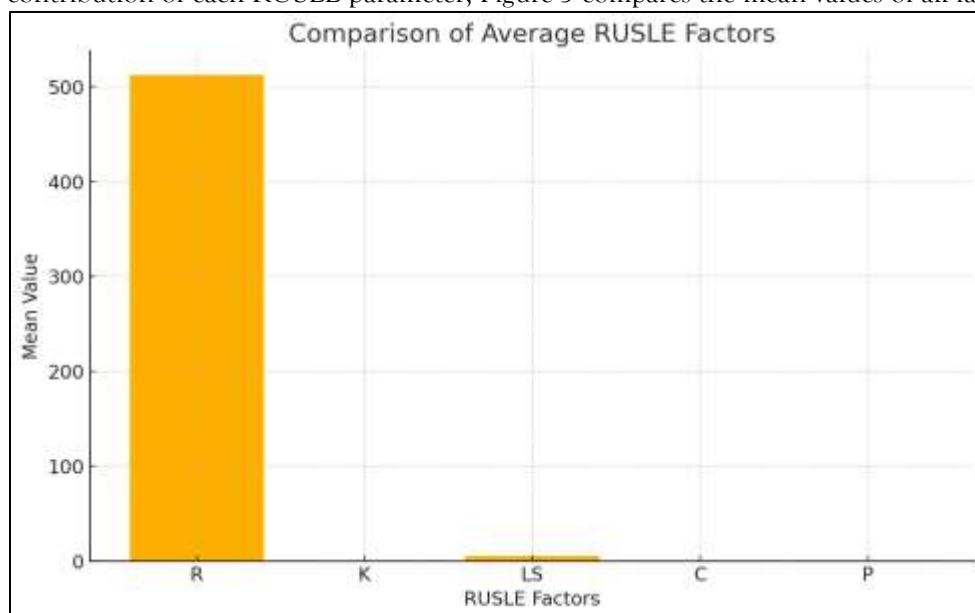


Figure 5 Comparison of Average RUSLE Factor Values

7.3 Identification and Characteristics of Erosion Hotspots

Erosion hotspot mapping identified clusters of high-risk zones primarily along concave channel bends, actively retreating riverbanks, and recently deposited floodplain surfaces. These hotspots represent areas undergoing rapid geomorphic adjustments, where high flow energy and sediment transport result in accelerated soil removal. Agricultural fields bordering the river margin also emerged as vulnerable, especially where seasonal cropping patterns leave soils bare during critical rainfall periods. The spatial alignment between hotspot locations and observed patterns of channel movement suggests that fluvial dynamics remain the most

dominant driver of severe erosion within the corridor. These findings highlight the necessity of targeted interventions in zones where geomorphological instability intersects with human land use. Figure 6 shows the statistical distribution of estimated annual soil loss values, reflecting substantial heterogeneity across the landscape.

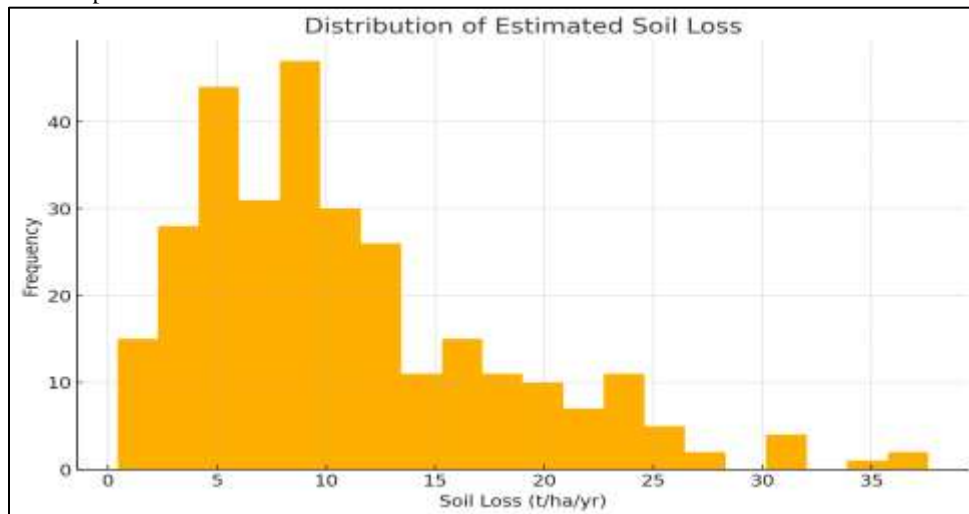


Figure 6 Soil Loss Distribution (Histogram)

7.4 Comparison with Previous Studies and Model Validation

The erosion patterns derived in this study are consistent with previous research findings for the Ganga basin and similar alluvial river systems worldwide. High erosion intensities near migrating channels and low slopes in vegetation-covered areas align with documented fluvial geomorphology. Validation using high-resolution satellite imagery and secondary field information suggests that the model captures both broad-scale and localized erosion characteristics effectively. While RUSLE inherently estimates long-term average erosion and may not account for extreme events, the model's integration with remote sensing data enhances its spatial resolution and reliability. The correspondence between model predictions and observed geomorphological conditions underscores the robustness of the RUSLE-GIS approach for regional erosion assessment. The relationship between terrain variables, vegetation cover, and erosion intensity is summarized in Figure 7, which shows clear contrasts among slope, NDVI, and soil loss distributions.

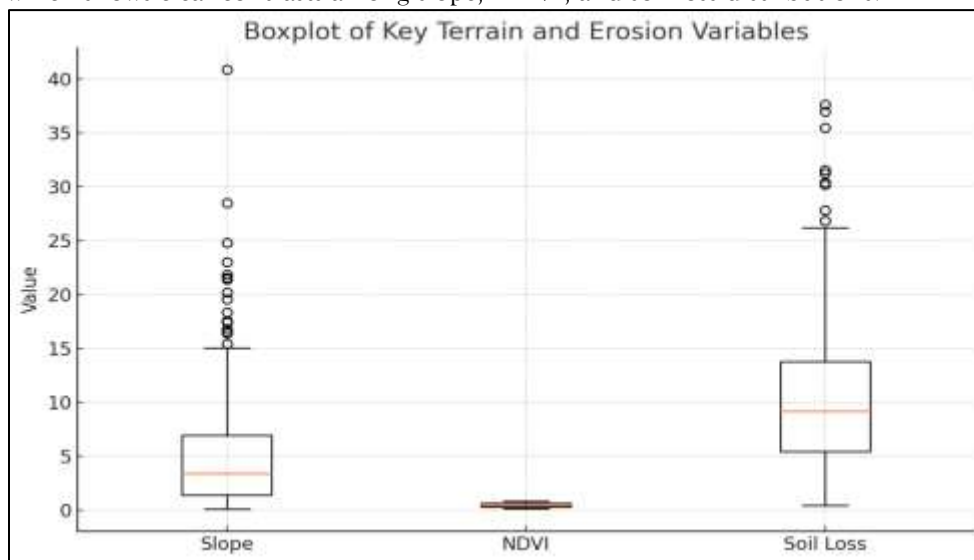


Figure 7 Boxplot of Slope, NDVI & Soil Loss

7.5 Implications for Land Management and Environmental Stability

The results have significant implications for sustainable land and water management in the Ganga River corridor. High erosion rates observed near agricultural settlements and riverbanks indicate potential threats

to soil fertility, agricultural productivity, and landscape stability. Accelerated erosion contributes to increased sediment loads in the river system, potentially affecting aquatic habitats, navigation, reservoir storage capacity, and downstream flood vulnerability. Socioeconomically, communities located in erosion-prone regions face risks of land loss, infrastructure damage, and displacement. These outcomes underscore the necessity for integrated erosion management strategies, incorporating both engineering and ecological approaches. The findings also emphasize the utility of remote sensing for continuous monitoring, enabling timely policy responses and adaptive management frameworks to mitigate future erosion impacts. As depicted in Figure 8, soil loss exhibits a strong positive association with slope magnitude, confirming the significant role of terrain steepness in controlling erosion risk.

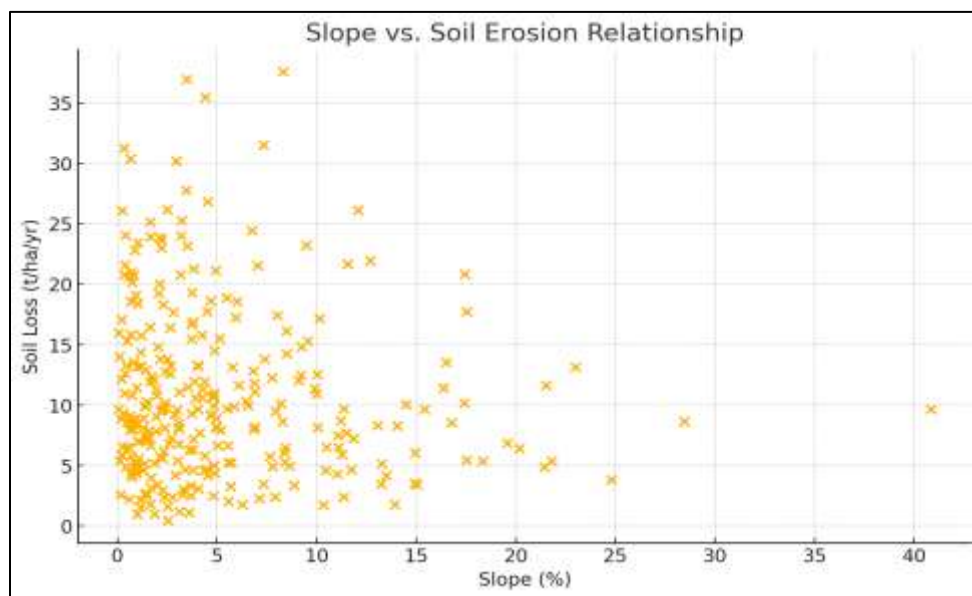


Figure 8 Scatter Plot (Slope vs. Soil Loss)

8. Management Strategies and Future Directions

8.1 Recommended Soil Conservation Measures

Mitigating soil erosion in the Ganga River corridor requires a strategic combination of biological, structural, and land-management interventions adapted to the region's geomorphic and hydrological context. Establishing continuous riparian buffer belts composed of deep-rooted native vegetation can significantly enhance riverbank stability and reduce direct erosive impacts of flowing water. On agricultural lands, conservation practices such as contour farming, no-till or reduced-till cultivation, mulching, and maintenance of crop residues are effective in reducing surface runoff and improving soil cohesion. The introduction of agroforestry systems and cover crops can further enhance soil organic matter and promote resilience against erosion. In zones where erosion is severe, especially along rapidly retreating riverbanks, engineered solutions such as vegetated geogrids, brushwood checks structures, revetments, and bioengineering methods provide necessary stabilization. Collectively, these measures support improved water infiltration, reduction in sediment detachment, and strengthening of ecological stability.

8.2 Policy-Level Considerations

Effective erosion mitigation must be supported by coherent policy frameworks that integrate environmental, agricultural, and land-management priorities. Policy mechanisms should discourage land-use expansion into high-risk erosion zones and foster responsible utilization of floodplains. Strict regulation of sand mining activities is essential to prevent destabilization of river channels and adjacent landscapes. Government-led incentive schemes promoting sustainable agricultural practices and soil conservation measures can encourage farmers to adopt erosion-control techniques. Additionally, policies should promote participatory watershed management approaches that involve local stakeholders in planning, implementation, and monitoring. A

coordinated river basin management framework, encompassing erosion control, water resource management, biodiversity protection, and disaster risk reduction, is critical for long-term sustainability.

8.3 Integration of Remote Sensing in Long-Term Monitoring

Remote sensing plays a pivotal role in establishing a robust, long-term monitoring system for soil erosion. Its capacity to provide regular, multi-temporal spatial data enables systematic tracking of land-use changes, vegetation dynamics, and channel migration. High-resolution satellite imagery, combined with machine learning algorithms and automated change-detection tools, can support near-real-time identification of emerging erosion hotspots. Integration of remote sensing with hydrological and sediment transport models enhances the predictive capabilities of erosion assessments. Furthermore, coupling satellite-based observations with ground surveys and UAV-based mapping can deliver comprehensive, multi-scale insights, facilitating adaptive management strategies and timely interventions.

8.4 Future Research Possibilities

Future research should explore advanced modeling approaches capable of capturing the complex interactions between climate variability, hydrological dynamics, and land-use change. The incorporation of climate projection data into erosion models will be essential for assessing future risk scenarios in the context of changing monsoon patterns and extreme weather events. High-resolution LiDAR and UAV-based photogrammetry offer promising avenues for detecting micro-topographic variations and evaluating small-scale erosion processes with enhanced precision. Interdisciplinary studies examining socio-economic drivers, community vulnerability, and behavioural responses to erosion can aid in designing more effective, community-centered mitigation strategies. Expanding spatial coverage to develop basin-wide erosion assessments and integrating digital twin concepts for dynamic simulation of riverine systems represent important future research directions.

9. REFERENCES

1. Aher, P. D., Adinarayana, J., & Gorantiwar, S. D. (2014). Quantification of soil erosion using RUSLE and GIS techniques: A case study of the Pravara River basin, India. *Applied Geomatics*, 6(3), 129–134.
2. Bera, K., & Bhattacharya, A. K. (2016). Soil erosion vulnerability assessment using geospatial technology: A study on the Ganga River basin in India. *Environmental Earth Sciences*, 75(3), 1–14.
3. Borrelli, P., Robinson, D. A., & Panagos, P. (2020). Land use and climate change impacts on global soil erosion by water (2015–2070). *Proceedings of the National Academy of Sciences*, 117(36), 21994–22001.
4. Brown, L. C., & Foster, G. R. (1987). Storm erosivity using idealized intensity distributions. *Transactions of the ASAE*, 30(2), 379–386.
5. Chakraborty, A., Joshi, P. K., & Singh, S. K. (2016). Spatial assessment of riverbank erosion of the Ganga River using remote sensing and GIS. *Geomorphology*, 257, 40–52.
6. De Roo, A. P. J., Wesseling, C. G., & Ritsema, C. J. (1996). LISEM: A single-event physically based hydrological and soil erosion model for drainage basins. *Hydrological Processes*, 10(8), 1107–1117.
7. Dutta, D., Kundu, A., & Patel, N. R. (2015). Predicting soil erosion potential of the Ganga River basin using RUSLE in GIS environment. *Journal of Earth System Science*, 124(6), 1343–1359.
8. Efe, S. I. (2016). Spatial variation in soil erosion risk using RUSLE model and GIS techniques in SW Nigeria. *Environmental Monitoring and Assessment*, 188(9), 1–17.
9. Ganasri, B. P., & Ramesh, H. (2016). Assessment of soil erosion by RUSLE model using remote sensing and GIS: A case study of Nethravathi Basin. *Geoscience Frontiers*, 7(6), 953–961.
10. Gupta, R., Tripathi, N. K., & Chauhan, H. B. (2019). Soil erosion modeling using RUSLE and GIS for a Himalayan watershed. *Environmental Earth Sciences*, 78(4), 1–14.
11. Lal, R. (2001). Soil degradation by erosion. *Land Degradation & Development*, 12(6), 519–539.
12. Lufafa, A., Tenywa, M. M., & Majaliwa, M. J. G. (2003). Prediction of soil erosion in a Lake Victoria basin catchment using RUSLE. *African Crop Science Journal*, 11(1), 55–64.
13. Mandal, U., & Sharda, V. N. (2013). Assessment of soil erosion in the Lower Ganga Basin using RUSLE and GIS. *Hydrological Sciences Journal*, 58(6), 1256–1269.
14. Millward, A. A., & Mersey, J. E. (1999). Adapting the RUSLE to model soil erosion potential in a mountainous tropical watershed. *CATENA*, 38(2), 109–129.
15. Mondal, M. S., & Jayaraman, V. (2015). Delineation of soil erosion prone areas using remote sensing and GIS: A case study of the Ganges delta. *Remote Sensing Applications*, 2, 21–30.
16. Morgan, R. P. C. (2005). *Soil erosion and conservation* (3rd ed.). Blackwell Publishing.
17. Nanda, A., & Goswami, R. (2020). Morphological changes and soil erosion assessment along the Ganga River using multi-temporal satellite data. *Remote Sensing in Earth Systems Sciences*, 3(1), 45–57.
18. Panagos, P., Borrelli, P., & Poesen, J. (2015). The European soil erosion map. *Science of the Total Environment*, 514, 318–325.

19. Patil, R. J., & Sharma, N. (2020). Estimation of soil loss using RUSLE and GIS: A case study of a Ganga sub-watershed. *Sustainable Water Resources Management*, 6, 1–13.
20. Rahman, M. R., & Siddiqua, S. (2018). Soil erosion hazard assessment using RUSLE and geospatial technology in a monsoon-dominated watershed. *Hydrology*, 5(3), 1–16.
21. Renard, K. G., Foster, G. R., Weesies, G. A., & Yoder, D. C. (1997). Predicting soil erosion by water: A guide to conservation planning with the Revised Universal Soil Loss Equation (RUSLE). USDA.
22. Sharma, A., Tiwari, K. N., & Bhadoria, P. B. S. (2011). Assessment of soil erosion by using RUSLE and remote sensing: A case study of Dhanbad district. *Journal of Geographic Information System*, 3(3), 267–276.
23. Singh, O., & Dubey, S. K. (2012). Modeling soil erosion risk in the Ganga Basin using RUSLE and GIS. *Journal of Hydrology and Environment Research*, 4(1), 35–47.
24. Srivastava, P., Shukla, A., & Mishra, V. (2021). Riverbank erosion susceptibility mapping of the Ganga River using geospatial techniques. *Natural Hazards*, 109, 1521–1542.
25. Wischmeier, W. H., & Smith, D. D. (1978). Predicting rainfall erosion losses: A guide to conservation planning. USDA Handbook No. 537.